Atmos. Chem. Phys. Discuss., 7, 14569–14601, 2007
www.atmos-chem-phys-discuss.net/7/14569/2007/

Atmospheric Chemistry and Physics Discussions

Global modeling of secondary organic aerosol formation from aromatic hydrocarbons: high- vs low-yield pathways

D. K. Henze[1], J. H. Seinfeld[1], N. L. Ng[1], J. H. Kroll[2], T. -M. Fu[3], D. J. Jacob[3], and C. L. Heald[4]

[1]Department of Chemical Engineering, California Institute of Technology, Pasadena, California, USA
[2]Aerodyne Research, Inc., Billerica, Massachusetts, USA
[3]School of Engineering and Applied Sciences and Department of Earth and Planetary Sciences, Harvard University, Cambridge, Massachusetts, USA
[4]Center for Atmospheric Sciences, University of California, Berkeley, California, USA

Received: 1 August 2007 – Accepted: 9 October 2007 – Published: 15 October 2007

Correspondence to: D. K. Henze (daven@caltech.edu)

Abstract

Formation of SOA from the aromatic species toluene, xylene, and, for the first time, benzene, is added to a global chemical transport model. A simple mechanism is presented that accounts for competition between low and high-yield pathways of SOA formation, wherein secondary gas-phase products react further with either nitrogen oxide (NO) or hydroperoxy radical (HO_2) to yield semi- or non-volatile products, respectively. Aromatic species yield more SOA when they react with OH in regions where the [NO]/[HO_2] ratios are lower. The SOA yield thus depends upon the distribution of aromatic emissions, with biomass burning emissions being in areas with lower [NO]/[HO_2] ratios, and the reactivity of the aromatic with respect to OH, as a lower initial reactivity allows transport away from industrial source regions, where [NO]/[HO_2] ratios are higher, to more remote regions, where this ratio is lower and, hence, the ultimate yield of SOA is higher. As a result, benzene is estimated to be the most important aromatic species with regards to formation of SOA, with a total production nearly equal that of toluene and xylene combined. In total, while only 39% percent of the aromatic species react via the low-NO_x pathway, 72% of the aromatic SOA is formed via this mechanism. Predicted SOA concentrations from aromatics in the Eastern United States and Eastern Europe are actually largest during the summer, when the [NO]/[HO_2] ratio is lower. Global production of SOA from aromatic sources is estimated at 3.5 Tg/yr, resulting in a global burden of 0.08 Tg, twice as large as previous estimates. The contribution of these largely anthropogenic sources to global SOA is still small relative to biogenic sources, which are estimated to comprise 90% of the global SOA burden, about half of which comes from isoprene. Compared to recent observations, it would appear there are additional pathways beyond those accounted for here for production of anthropogenic SOA. However, owing to differences in spatial distributions of sources and seasons of peak production, there are still regions in which aromatic SOA produced via the mechanisms identified here are predicted to contribute substantially to, and even dominate, the local SOA concentrations, such as outflow regions from North America

ACPD

7, 14569–14601, 2007

and South East Asia during the wintertime, though total SOA concentrations there are small (~0.1 μg/m^3).

1 Introduction

Organic aerosols play an important role in global climate (Kanakidou et al., 2005). A significant fraction of organic aerosol material results from the gas-phase oxidation of volatile hydrocarbons to yield semivolatile products that condense into the particulate phase; this is referred to as secondary organic aerosol (SOA). At present, levels of organic aerosol measured in field campaigns tend to exceed those predicted by global chemical transport models (Heald et al., 2005, 2006). While it is predicted that, on the global scale, secondary organic aerosol from biogenic sources substantially exceeds that from anthropogenic sources (Tsigaridis et al., 2006; Tsigaridis and Kanakidou, 2007), data from recent field studies suggest that SOA from anthropogenic hydrocarbons might be more significant than previously thought (de Gouw et al., 2005; Volkamer et al., 2006).

Among anthropogenic hydrocarbons, aromatic compounds are generally considered to be the most important SOA precursors. It has recently been established that the SOA yields (aerosol yield is defined as the ratio of the mass of organic aerosol produced to the mass of parent hydrocarbon reacted) from aromatics, as well as those from a variety of other hydrocarbons, depend critically on the prevailing level of nitrogen oxides (NO_x) (Hurley et al., 2001; Martin-Reviejo and Wirtz, 2005; Presto et al., 2005; Song et al., 2005; Johnson et al., 2004, 2005; Ng et al., 2007). This discovery led to a systematic re-evaluation of aromatic SOA yields (Ng et al., 2007) from the historical yields of Odum et al. (1996, 1997) that were measured under high-NO_x conditions. In particular, aromatic yields under the low-NO_x conditions typical of most of the global atmosphere significantly exceed those under high-NO_x conditions typical of urban cores (and of past laboratory chamber experiments). However, given that sources of aromatics are likely co-located with sources of NO_x, the significance of this

ACPD
7, 14569–14601, 2007

EGU

finding on the global SOA burden is not readily apparent.

Initial global modeling studies of SOA formation from toluene and xylene (Tsigaridis and Kanakidou, 2003) used the empirical yield parameters from Odum et al. (1996, 1997). More recently, this model was updated to include the NO_x dependence of yields for toluene and xylene based upon the xylene yields in the work of Song et al. (2005). Lack et al. (2004) also included aromatic species in their lumped calculation of SOA formation from industrial sources, using yield coefficients from (Odum et al., 1997) and (Cocker et al., 2001). Calculation of SOA formation from benzene has been identified in the box model studies of Pun and Seigneur (2007) as an important additional pathway. The recent data (Ng et al., 2007) on SOA yields from all of these aromatic hydrocarbons prompt a re-evaluation of the contribution of aromatic SOA to the global SOA production rate and burden. In the current study, the GEOS-Chem global chemical transport model is updated to include abbreviated aromatic oxidation chemistry and SOA formation from aromatics.

2 Summary of SOA yields from aromatic hydrocarbons

The SOA-forming potentials of *m*-xylene, toluene, and benzene have been measured in a series of laboratory chamber experiments (Ng et al., 2007). Atmospheric reaction of these aromatics with the hydroxyl radical (OH) initiates a complex series of gas-phase reactions (Calvert et al., 2002; Koch et al., 2007). As noted above, a crucial factor governing the nature of the gas-phase chemistry and subsequent aerosol formation is the NO_x level. Experiments were conducted under both low- and high-NO_x conditions; these correspond to NO_x levels of less than 1 parts-per-billion by volume (ppb) and several hundred ppb, respectively.

SOA yields of the three aromatics studied are highly dependent on the prevailing NO_x level. Under high-NO_x conditions, measured yields for toluene and *m*-xylene are in the range of 5 to 10% with a strong dependence on the amount of organic aerosol present, in general agreement with those reported by Odum et al. (1996, 1997). Under low-

NO_x conditions, all three compounds exhibit high (≥30%) constant yields, exceeding yields from high-NO_x conditions. The first studies of SOA yields from benzene reported yields in the range of 10% for both high and low-NO_x conditions (Martin-Reviejo and Wirtz, 2005); Ng et al. (2007) found a considerably higher yield for benzene, 28% under high-NO_x conditions. The discrepancies between the two reported low-NO_x yields in (Martin-Reviejo and Wirtz, 2005) and the one yield in Ng et al. (2007) may be a result of higher SOA yields in the presence of an inorganic seed in the experiments of Ng et al. (2007). Additional factors, such as the uncertainty in the benzene threshold concentrations in Martin-Reviejo and Wirtz (2005) make comparisons between these results difficult. While additional studies of the low-NO_x yields of benzene are clearly called for, use of inorganic seed particles in Ng et al. (2007) affords decoupling of the NO_x effect from the effects of an "induction period" caused in their absence (Kroll et al., 2007), which will be shown to facilitate use of such data for modeling SOA formation.

The mechanisms for atmospheric oxidation of both biogenic and anthropogenic hydrocarbons are complex and not fully understood; it does appear, however, that the observed low- and high-NO_x behavior of SOA formation (Song et al., 2005; Ng et al., 2007) hinges on the competitive reactions of the bicyclic peroxy radicals ($ROHO_2$) that result from initial attack of the aromatic species (R) by OH radicals followed quickly by O_2 addition and cyclization (Johnson et al., 2005; Koch et al., 2007), written here simply as

$$R + OH\cdot \xrightarrow{k_{OH}} \dot{R}OH \xrightarrow{O_2} ROHO_2\cdot . \quad \text{(R1)}$$

As explained in detail in Ng et al. (2007), the alternative reaction of the aromatic-OH adduct with NO_2 is not expected to play a significant role in the chamber conditions (Koch et al., 2007), nor are levels of NO up to ppm expected to prevent formation of the bicyclic peroxy radical from its isomer that initially results from O_2 addition (Zhao et al., 2005; Fan and Zhang, 2006). The peroxy radicals react predominantly with either hydroperoxy radicals (HO_2) or NO, depending on the relative concentrations of HO_2 and NO. Reaction of the peroxy radicals with themselves is found to be unimportant under

chamber conditions (the rate constant for this is relatively small and HO_2 concentrations are high) in the kinetic simulations of Ng et al. (2007). The role of such competing reactions in the atmosphere is assessed later in the present work.

While it is common to refer to the oxidative conditions in environmental chambers according to absolute NO_x levels or VOC:NO_x ratios (as those are typically what is measured), it is often the ratio of [NO]/[HO_2] that determines the fate of secondary gas-phase products and which is more important than absolute NO_x concentrations for extrapolating results from environmental chamber conditions to atmospheric conditions. Under low-NO_x conditions, the levels of HO_2 radical in the chamber are such that reaction with HO_2 radical is favored, and the resulting products, including hydroperoxides, are generally less volatile than those that result from the NO reaction path. This competition can be represented as follows:

$$\mathrm{ROHO_2}\cdot + \mathrm{HO_2}\cdot \xrightarrow{k_H} \alpha_H \mathrm{SOG}_H + \cdots \quad \text{(R2)}$$

$$\mathrm{ROHO_2}\cdot + \mathrm{NO} \xrightarrow{k_N} \alpha_1 \mathrm{SOG}_1 + \alpha_2 \mathrm{SOG}_2 + \cdots \quad \text{(R3)}$$

where SOG designates secondary organic gas-phase semivolatile products, and the α's are mass-based stoichiometric coefficients (i.e. for every gram of peroxy radical that reacts, α grams of SOG are formed).

The fact that, for all three aromatics, the SOA yield under low-NO_x conditions is constant with respect to changes in available substrate implies that the semivolatile products are essentially nonvolatile, at least at the level of aerosol mass concentrations in the chamber; thus, the $ROHO_2$+HO_2 pathway can be represented as leading to a single nonvolatile product, SOG_H=SOA_H. Since the high-NO_x pathway exhibits yields that depend on the total amount of absorbing organic aerosol, we use the customary two-product model for SOA formation, originally formulated by Odum et al. (1996, 1997); SOG_1 and SOG_2 represent these products, which have associated gas-particle

partitioning equilibrium constants, K_1 and K_2,

$$[\mathrm{SOG}_j] = \frac{[\mathrm{SOA}_j]}{K_j M},$$

where M is the concentration of total available substrate in $\mu\mathrm{g\,m^{-3}}$. Parameters describing yields under both sets of NO_x levels are given in Table 1. Equilibrium constants and stoichiometric coefficients are based on laboratory studies of Ng et al. (2007), where here the latter are multiplied by the ratio of the molecular weight of the parent aromatic to that of the peroxy radical to reflect formation of SOG species directly from the peroxy radical. The assumption that the low-NO_x product is nonvolatile is specific to aromatic species; in general, sets of α's and K's can be derived for semivolatile products from both pathways.

3 Aromatic SOA formation in GEOS-Chem

In the current study, the GEOS-Chem global chemical transport model (version 7-04-11 with a horizontal resolution of 2°×2.5° and 30 layers up to 0.01 hPa, GEOS-4 meteorological fields) is used to simulate one year of present day conditions (2004). This model includes detailed simulation of gas-phase tropospheric chemistry (e.g., Bey et al., 2001; Hudman et al., 2007) in addition to external mixtures of several aerosol components (Park et al., 2004, 2006). Previous versions have been implemented with a gas-particle partitioning model of SOA formation from terpenes, alcohols, sesquiterpenes (Chung and Seinfeld, 2002; Heald et al., 2005) and isoprene (Henze and Seinfeld, 2006). As such, estimates of organic carbon aerosol have been notably low compared to measurements during springtime 2001 measurements in the free troposphere of the Asian continental outflow region (ACE-Asia) (Heald et al., 2005) and have failed to capture the variance in observations in the free troposphere during the summer 2004 campaign (ICARTT) in the northeastern United States (Heald et al., 2006);

ACPD
7, 14569–14601, 2007

EGU

in comparison, such overwhelming inconsistencies have not been found in yearly average estimates of surface organic aerosol concentrations compared to filter samples (Liao et al., 2007). The addition of abbreviated aromatic oxidation chemistry and SOA formation from aromatics to the chemical reactions and SOA module in GEOS-Chem is described in the following sections.

3.1 Aromatic global emissions

Global emissions of benzene, toluene and xylene from industrial and fossil fuel sources are taken from the Emission Database for Global Atmospheric Research (EDGAR V2.0) (Olivier et al., 1996, 1999) for 1990 and scaled to the year 2000 using liquid fossil fuel usage from the Global Emission Inventory Activity (GEIA) project (Benkovitz et al., 1996) following Bey et al. (2001). Emissions of aromatics from biofuel and biomass burning are calculated by applying emission ratios to emissions of CO, where sources of CO from biofuel burning are from the GEIA database, while biomass burning sources of CO are from the Global Fire Emissions Database version 2 (GFEDv2) (Giglio et al., 2006; van der Werf et al., 2006). The emissions ratios, listed in Table 3, are taken from Andreae and Merlet (2001) with updates from M. O. Andreae (personal communication, 2006). Total emissions are 5.6, 6.9 and 4.7 Tg C/yr for benzene, toluene and xylene, respectively. The breakdown by source type is given in Table 4, and the yearly average emission fluxes of each aromatic species, and the combined total, are shown in Fig. 1. The largest global sources are road transport and solvent use (for toluene and xylene), and biofuel and biomass burning (for benzene); road transport is the main source of benzene in urban areas.

3.2 Implementation of aromatic SOA formation

Gas-phase oxidation of each parent aromatic hydrocarbon (R1) and subsequent reaction of the peroxy radical product with HO_2 (R2) and NO (R3) is calculated online as an additional part of the tropospheric chemical reaction mechanism. By explicitly cal-

culating the branching ratio between these two pathways, this implementation allows natural transitions between low and high-yield environments as governed by temperature, and HO_2 radical and NO concentrations. This approach, initially suggested in the work of Presto and Donahue (2006), has the advantage of avoiding prior delineation of oxidative regimes based upon VOC/NO_x ratios (Song et al., 2005; Tsigaridis et al., 2006; Presto and Donahue, 2006). Parameters for calculating the reaction rate constants for these steps are listed in Table 2. Kinetic parameters for reaction of the aromatic species with OH (the rate limiting step in peroxy radical formation) are from Calvert et al. (2002). Rate constants for peroxy radical reactions, (R2) and (R3), are from Atkinson et al. (1997), assuming similar temperature dependence as peroxy radical reactions with isoprene, as most reactions of hydrocarbons with NO and HO_2 have similar kinetics (Lightfoot et al., 1992; Eberhard and Howard, 1997). All forms of xylene are assumed to behave as *m*-xylene for both gas and aerosol processes.

Calculation of reversible SOA formation follows the approach outlined in Chung and Seinfeld (2002). The empirical yield parameters (Table 1) are used to estimate the mass of SOA formed per mass of peroxy radical that reacts. An important aspect of this treatment is specification of the available substrate, M, which affects gas-particle equilibrium. For this work, M is taken to consist of the total mass of primary and secondary organic material.[1] As GEOS-Chem tracks only the carbonaceous component of primary organic aerosol, the ratio of organic to total carbon aerosol mass must be specified in order to calculate M – here the ratio is assumed to be 2.1. Though this differs from previous studies that used a ratio of 1.4 (Henze and Seinfeld, 2006; Liao et al., 2007; Heald et al., 2006; Zhang et al., in press; van Donkelaar et al., 2007), 2.1 is recommended for non-urban aerosols (Turpin and Lim, 2001). This adjustment alone causes a nearly 20% increase in total SOA production; hence, specification of the carbon content of SOA is clearly an important source of uncertainty in these calculations. The Clausius-Clapeyron equation is used to extrapolate equilibrium constants

[1] Condensation directly on sulfate aerosol, considered in some versions of GEOS-Chem and other studies (Tsigaridis and Kanakidou, 2003), is not included in these simulations.

to tropospheric temperatures. The enthalpy of vaporization for SOA, a major source of uncertainty in such calculations (Tsigaridis and Kanakidou, 2003; Henze and Seinfeld, 2006), is assumed to be 42 kJ mol^{-1} for all species, in the range of limited available experimental data (Offenberg et al., 2006). Dry deposition of all types of SOA is calculated using a resistance-in-series model (Wesely, 1989; Wang et al., 1998); wet scavenging follows Liu et al. (2001) with an assumed scavenging efficiency of 80% (Chung and Seinfeld, 2002).

Additional sources of uncertainty include the extent to which yields determined in chamber studies in the presence of high organic aerosol loadings (~30 μg m^{-3}) can be extrapolated to the atmosphere (Presto and Donahue, 2006; Pathak et al., 2007), particularly given the assumption of irreversible SOA formation at low NO_x. Further, the low-NO_x yield parameters for benzene were fit to a time series of data points from a single photooxidation experiment in Ng et al. (2007) which, while well suited for cleanly assessing the SOA yields via Reaction (R2), await additional experimental verification. Finally, as noted previously, application of this abbreviated mechanism for aromatic oxidation chemistry does not include reaction of the peroxy radicals with themselves, a pathway for which SOA yields are not known, nor reaction of the aromatic-OH adduct with NO_2 instead of O_2. With average concentrations of NO_2 in the 2°×2.5° grid cells of the global model used here being <100 ppb, reaction of the aromatic-OH adduct with NO_2 is not likely an important pathway (Volkamer et al., 2002; Koch et al., 2007). Self reaction of peroxy radicals may be an important reaction in areas where the peroxy radical concentrations exceed those of NO and HO_2 by much more than an order of magnitude as the rate constant at 298 K is slower (likely $<1 \times 10^{-14}$ cm^3 molecule^{-1} s^{-1} given their level of substitution) than k_N (8.5×10^{-12} cm^3 molecule^{-1} s^{-1}) or k_H (1.5×10^{-11} cm^3 molecule^{-1} s^{-1}). However, this may be rare since estimated concentrations of even the parent aromatic species are typically on the order of only a few ppb near source regions, where NO_x concentrations are of order 0.1 ppb and/or HO_2 are 10 ppt.

ACPD
7, 14569–14601, 2007

4 Simulation of global aromatic SOA

The predicted contributions of benzene, toluene, and xylene to global aromatic SOA via high- and low-yield pathways (the opposite of the NO_x levels) and the percentage of the aromatics that react via each pathway are given in Fig. 2. Thus, 51% of globally emitted benzene, for example, reacts via Reaction (R2), the high-yield path, whereas only 26% of xylene follows this route. The location of the sources plays an important role in determining the total SOA yield from each species. Aromatics, primarily benzene, emitted from biofuel and biomass burning sources are more likely to react via the high-yield pathway as these emissions are less associated with sources of NO_x than the industrial and fossil fuel emissions. Additionally, for emissions from industrial and fossil fuel sources, it is the less reactive aromatics, as measured by their OH reaction rate constants, that actually produce more SOA. The explanation is that lower reactivity affords the parent hydrocarbon more time to be transported to regions of lower [NO]/[HO_2] ratios, where ultimately, once reacted, the SOA yield is larger. Proportionately more of a reactive molecule like xylene is consumed in regions in which the NO_x levels are more characteristic of the source emission areas. On a global average, 39% of the total aromatics proceed through the high yield pathway. As a result, 72% of global aromatic SOA is produced via the high-yield (low-NO_x) pathway.

Figure 3 shows the predicted seasonally averaged surface-level concentrations of aromatic SOA. The concentrations generally reflect the distribution of areas with substantial anthropogenic emissions in northern mid-latitudes, which are themselves aseasonal, and biomass burning in the Southern Hemisphere, which have strong seasonal cycles. The resulting SOA concentrations show considerable seasonal variability, even in the northern mid-latitudes. Concentrations in the eastern parts of the United States and Europe are lowest during the Northern Hemisphere winter months, and highest during the Northern Hemisphere summer months. Figure 4 shows the contrast between the estimated concentrations of NO and HO_2 radical during DJF and JJA, the cycles of which both contribute to more of the aromatics in these areas reacting via the

high-yield pathway during the summer. The combined effects on the fate of toluene are shown in panels (e) and (f), which are the log of the branching ratio,

$$\log_{10}\left(\frac{\text{Number of toluene peroxy radicals that proceed via reaction with NO}}{\text{Number of toluene peroxy radicals that proceed via reaction with HO}_2}\right).$$

For example, yellow colors indicate areas where the NO pathway is estimated to dominate by two or more orders of magnitude while blue colors indicate areas where an order of magnitude more toluene molecules are calculated to proceeded via the HO_2 pathway. Values where the total toluene peroxy radical concentrations are less that 1% of the maximum global surface concentration are not shown. The HO_2 pathway entirely dominates only rarely; however, it is clear that SOA formation via this low-NO_x pathway is much more important in the eastern United States and Europe during JJA than DJF. Also note that during JJA, SOA production in these areas is not inhibited by increased summertime temperatures as formation of SOA via the low-NO_x pathway is treated as irreversible. Biogenic sources of organic aerosol are also elevated during the summer. This additional substrate increases SOA production from aromatics via the (R3) pathway, but this enhancements is found to be less than 5%. This demonstrates the potential of NO_x variations, whether perturbed by changes in anthropogenic emissions or modulated by natural seasonal cycles, to influence global SOA yields.

Total aromatic emissions and resulting SOA production rates and burdens are given in Table 5. The burden of SOA from aromatic compounds is estimated here to be 0.08 Tg. Similarly, recent work by Tsigaridis and Kanakidou (2007) estimated SOA burdens from aromatics at 0.04 Tg, considering only toluene and xylene. Using the same yields and mechanism reported here, Heald et al. (2007)[2] explored the response of SOA estimates to future climate, land-use and emissions changes in a general circulation model and estimated present day production of SOA from anthropogenic sources

[2]Heald, C. L., Henze, D. K., Horowitz, L. W., et al.: Predicted change in global secondary organic aerosol concentrations in response to future climate, emissions, and land-use change, submitted, 2007.

to be 3.4 Tg C/yr. Each of these studies highlights the importance of accounting for the NO_x dependent yields of these species. Overall, the range of estimated global burdens of aromatic SOA from recent simulations (0.04–0.10 Tg) is more than twice as high as earlier estimates of 0.01–0.03 Tg (Tsigaridis and Kanakidou, 2003).

5 Anthropogenic vs biogenic SOA

Table 5 also presents the emissions and resulting production rates and burdens of SOA from biogenic species, where for simplicity we consider all aromatic sources to be anthropogenic, though undoubtedly some of the biomass burning sources are naturally occurring. Even though aromatic SOA is appreciable, the global SOA burden is dominated by biogenic sources, about 50% of which is attributable to isoprene, as predicted based on current SOA yields from laboratory chamber studies. As such, addition of aromatic SOA does not significantly affect global estimates of biogenic SOA through nonlinear effects, though it may have a stronger influence in future emissions scenarios (Tsigaridis and Kanakidou, 2007, and Heald et al., 2007[2]).

While the bulk of the total modeled SOA is biogenic in origin, there are regions of the global distribution where concentrations of SOA from aromatics are predicted to be equal or larger. Figure 5 shows the log of the ratio of aromatic to biogenic SOA concentrations,

$$\log_{10}\left(\frac{[\mathrm{SOA}_{\mathrm{arom}}]}{[\mathrm{SOA}_{\mathrm{biogenic}}]}\right)$$

excluding locations where the total SOA concentration is less than 0.05 μg/m^3. During DJF and MAM, much of the outflow regions in the Northern Hemisphere are dominated by anthropogenic SOA. Nevertheless, SOA concentrations in these areas are still small, <0.1 μg/m^3, as can be seen by comparison to Fig. 3. Further, concentrations in these regions are typically much smaller than the total (primary plus secondary)

organic aerosol. For example, Fig. 6 shows the profile of SOA concentrations at 70° W, an area identified in Fig. 5 where the SOA is predominantly anthropogenic in origin. While SOA concentrations from aromatics, see panel (a), are greater than from other sources, panel (b), the total SOA concentrations are small, particularly in comparison to total carbon aerosol concentrations, panels (c)–(d). As such, the revised estimates of total carbonaceous aerosol from this work alone do not likely explain the "missing source" of SOA noted in previous model estimates of OC aerosol in ACE-Asia (Heald et al., 2005), nor the magnitude and variability of soluble OC from observations during the ICARTT campaign of summer, 2004 (Heald et al., 2006). Over the Northeastern United States during JJA, the estimated SOA from aromatics via the pathways considered here is still smaller than the anthropogenic source of SOA suggested by de Gouw et al. (2005). While it is tempting to directly compare the results of the present calculation to the observations of SOA formation in Mexico City reported by Volkamer et al. (2006), the results of this global modeling study are too coarse to resolve specific urban scale pollution events, and the NO_x levels in such cases can greatly exceed those within the regime covered by the global model developed here. However, it would appear that additional mechanisms for anthropogenic SOA formation still exist beyond those presently considered.

6 Conclusions

The global chemical transport model GEOS-Chem is updated to include simulation of SOA formation from the aromatic species benzene, toluene and xylene. Following the suggestion of Presto and Donahue (2006), a simple mechanism is presented that accounts for the competition between low and high-NO_x pathways on SOA formation in a continuous fashion. Depending upon the immediate chemical environment, secondary peroxy radicals from photooxidation of aromatics by OH react with either NO or HO_2 radical. Formation of SOA from reaction with NO leads to reversible formation of SOA following the two-product model of Odum et al. (1996, 1997) using empirically deter-

mined yield and partitioning coefficients from the high-NO_x studies of Ng et al. (2007). Aromatic peroxy radicals that react with HO_2 radical are treated as forming SOA irreversibly, following the low-NO_x results of Ng et al. (2007). This approach to treating NO_x dependence is general and could (with enough empirical data) be extended to address the NO_x dependence of other species that are associated enough with sources of NO_x to warrant discrimination between the two pathways. For the aromatic species, explicitly considering both pathways was found to be important as substantial amounts (25% or higher) of each aromatic species proceed via each pathway. In contrast, implementing a similar model description for monoterpenes or isoprene, largely emitted in low-NO_x environments, may not be as crucial for estimating their global contributions to SOA.

Previously assumed to generate negligible amounts of SOA because of its low reactivity with OH, benzene is estimated in this work to be the most important aromatic species with regards to formation of SOA owing to its low initial reactivity and the location of its emissions. Its low initial reactivity allows benzene to be transported away from source regions, where [NO]/[HO_2] ratios are high, to more remote regions, where this ratio is lower and, hence, the ultimate yield of SOA is higher. In total, nearly 75% of the aromatic SOA is formed via the low-NO_x pathway, though only 39% percent of the aromatic species react via this mechanism. Predicted SOA concentrations from aromatics in the Eastern United States and Europe are actually largest during the summer, owing to both higher HO_2 radical concentrations and lower NO concentrations. Influence of NO_x variability on SOA formation is particularly interesting as current models may underestimate seasonal NO_x cycles in many areas as indicated by observations from GOME (van Noije et al., 2006; Wang et al., 2007), though further analysis is warranted.

Even though the predicted burden and production rate of aromatic SOA is twice that of previous estimates (Tsigaridis and Kanakidou, 2003, 2007), the contribution of these sources to global SOA is small relative to contributions from monoterpenes and isoprene, which alone are estimated to comprise 82% of the global SOA burden. However, owing to differences in spatial distributions of sources and seasons of peak

production, there are regions in which aromatic SOA is predicted to contribute substantially to, and even dominate, the local SOA concentrations, such as outflow regions from North America and South East Asia during the wintertime. The contribution of aromatic SOA to carbonaceous aerosol may also affect interpretation of total organic carbon aerosol concentrations from surface stations in which winter concentrations have been assumed to be primary in origin (Liao et al., 2007).

Overall, comprehensive model treatment of SOA is still difficult owing to a large range of effects not yet included, from interactions of aqueous and organic phases (Pun and Seigneur, 2007) to effects of particle acidity on yields from isoprene (Surratt et al., 2007). Uncertainties in biogenic emissions estimates are frequently cited; uncertainties of even the aromatic emissions are possibly as large as a factor of two or more (Warneke et al., 2007). Recent works by Presto and Donahue (2006) and Pathak et al. (2007) also emphasize the importance of accounting for other effects, such as low aerosol mass loading, when parameterizing SOA yields from chamber data; all of these topics will be important areas of future research and model development. Additional mechanisms beyond those presented here may play important roles in production of SOA from aromatic species. However, the importance of NO_x on estimating yields of SOA from aromatics is clear. This work highlights the importance of additional studies of the NO_x dependence of SOA formation from other species, and the role that such dependance plays on SOA yields of long lived hydrocarbons in general, as this represents an important mechanism by which anthropogenic activity can affect global SOA. This is of concern for not only interpretation of current measurements of organic aerosol, but also for estimates of the effects of future climate and emissions changes on global aerosol burdens (Tsigaridis and Kanakidou, 2007, Heald et al., 2007[2]).

Acknowledgements. This work was supported by U.S. Environmental Protection Agency, grant R832158, and the National Science Foundation, grant NSF ITR AP&IM 0205198, which provided access to the TeraGrid resources at the National Center for Supercomputing Applications.

References

Andreae, M. O. and Merlet, P.: Emission of trace gases and aerosols from biomass burning, Global Biogeochem. Cy., 15, 955–966, 2001. 14576, 14593

Atkinson, R., Baulch, D. L., Cox, R. A., Hampson, R. F., Kerr, J. A., Rossi, M. J., and Troe, J.: Evaluated kinetic and photochemical data for atmospheric chemistry: Supplement VI - IUPAC subcommittee on gas kinetic data evaluation for atmospheric chemistry, J. Phys. Chem. Ref. Data, 26, 1329–1499, 1997. 14577

Benkovitz, C. M., Scholtz, M. T., Pacyna, J., Tarrason, L., Dignon, J., Voldner, E. C., Spiro, P. A., Logan, J. A., and Graedel, T. E.: Global gridded inventories of anthropogenic emissions of sulfur and nitrogen, J. Geophys. Res., 101, 29 239–29 253, 1996. 14576

Bey, I., Jacob, D. J., Yantosca, R. M., Logan, J. A., Field, B. D., Fiore, A. M., Li, Q. B., Liu, H. G. Y., Mickley, L. J., and Schultz, M. G.: Global modeling of tropospheric chemistry with assimilated meteorology: Model description and evaluation, J. Geophys. Res., 106, 23 073–23 095, 2001. 14575, 14576

Calvert, J., Atkinson, R., Becker, K. H., Kamens, R. M., Seinfeld, J. H., Wallington, T. J., and Yarwood, G.: The mechanisms of atmospheric oxidation of aromatic hyrdocarbons, Oxford University Press, New York, 2002. 14572, 14577

Chung, S. H. and Seinfeld, J. H.: Global distribution and climate forcing of carbonaceous aerosols, J. Geophys. Res., 107, 4407, doi:10.1029/2001JD001397, 2002. 14575, 14577, 14578

Cocker, D. R., David, R., Mader, B. T., Kalberer, M., Richard, C., and Seinfeld, J. H.: The effect of water on gas-particle partitioning of secondary organic aerosol, II, *m*-xylene and 1, 3, 5-trimethylbenzene photooxidation systems, Atmos. Environ., 35, 6073–6085, 2001. 14572

de Gouw, J. A., Middlebrook, A. M., Warneke, C., Goldan, P. D., Kuster, W. C., Roberts, J. M., Fehsenfeld, F. C., Worsnop, D. R., Canagaratna, M. R., Pszenny, A. A. P., Keene, W. C., Marchewka, M., Bertman, S. B., and Bates, T. S.: Budget of organic carbon in a polluted atmosphere: Results from the New England Air Quality Study in 2002, J. Geophys. Res., 110, D16305, doi:10.1029/2004JD005623, 2005. 14571, 14582

Eberhard, J. and Howard, C. J.: Rate coefficients for the reactions of some C-3 to C-5 hydrocarbon peroxy radicals with NO, J. Phys. Chem. A, 101, 3360–3366, 1997. 14577

Fan, J. W. and Zhang, R. Y.: Atmospheric oxidation mechanism of p-xylene: A density functional theory study, J. Phys. Chem. A, 110, 7728–7737, 2006. 14573

Giglio, L., van der Werf, G. R., Randerson, J. T., Collatz, G. J., and Kasibhatla, P.: Global estimation of burned area using MODIS active fire observations, Atmos. Chem. Phys., 6, 957–974, 2006, http://www.atmos-chem-phys.net/6/957/2006/. 14576

Heald, C. L., Jacob, D. J., Park, R. J., Russell, L. M., Huebert, B. J., Seinfeld, J. H., Liao, H., and Weber, R. J.: A large organic aerosol source in the free troposphere missing from current models, Geophys. Res. Lett., 32, L18809, doi:10.1029/2005GL023831, 2005. 14571, 14575, 14582

Heald, C. L., Jacob, D. J., Turquety, S., Hudman, R. C., Weber, R. J., Sullivan, A. P., Peltier, R. E., Atlas, E. L., de Gouw, J. A., Warneke, C., Holloway, J. S., Neuman, J. A., Flocke, F. M., and Seinfeld, J. H.: Concentrations and sources of organic carbon aerosols in the free troposphere over North America, J. Geophys. Res., 111, D23S47, doi:10.1029/2006JD007705, 2006. 14571, 14575, 14577, 14582

Henze, D. K. and Seinfeld, J. H.: Global secondary organic aerosol from isoprene oxidation, Geophys. Res. Lett., 33, L09812, doi:10.1029/2006GL025976, 2006. 14575, 14577, 14578

Hudman, R. C., Jacob, D. J., Turquety, S., Leibensperger, E. M., Murray, L. T., Wu, S., Gilliland, A. B., Avery, M., Bertram, T. H., Brune, W., Cohen, R. C., Dibb, J. E., Flocke, F. M., Fried, A., Holloway, J., Neuman, J. A., Orville, R., Perring, A., Ren, X., Sachse, G. W., Singh, H. B., Swanson, A., and Wooldridge, P. J.: Surface and lightning sources of nitrogen oxides over the United States: magnitudes, chemical evolution, and outflow, J. Geophys. Res., 112, D12S05, doi:10.1029/2006JD007912, 2007. 14575

Hurley, M. D., Sokolov, O., Wallington, T. J., Takekawa, H., Karasawa, M., Klotz, B., Barnes, I., and Becker, K. H.: Organic aerosol formation during the atmospheric degradation of toluene, Environ. Sci. Technol., 35, 1358–1366, 2001. 14571

Johnson, D., Cassanelli, P., and Cox, R. A.: Isomerization of simple alkoxyl radicals: New temperature-dependent rate data and structure activity relationship, J. Phys. Chem. A, 108, 519–523, 2004. 14571

Johnson, D., Jenkin, M. E., Wirtz, K., and Martin-Reviejo, M.: Simulating the formation of secondary organic aerosol from the photooxidation of aromatic hydrocarbons, Environ. Chem., 2, 35–48, 2005. 14571, 14573

Kanakidou, M., Seinfeld, J. H., Pandis, S. N., Barnes, I., Dentener, F. J., Facchini, M. C., Van Dingenen, R., Ervens, B., Nenes, A., Nielsen, C. J., Swietlicki, E., Putaud, J. P., Balkanski, Y., Fuzzi, S., Horth, J., Moortgat, G. K., Winterhalter, R., Myhre, C. E. L., Tsigaridis, K.,

Vignati, E., Stephanou, E. G., and Wilson, J.: Organic aerosol and global climate modelling: a review, Atmos. Chem. Phys., 5, 1053–1123, 2005, http://www.atmos-chem-phys.net/5/1053/2005/. 14571

Koch, R., Knispel, R., Elend, M., Siese, M., and Zetzsch, C.: Consecutive reactions of aromatic-OH adducts with NO, NO2 and O-2: benzene, naphthalene, toluene, m- and p-xylene, hexamethylbenzene, phenol, m-cresol and aniline, Atmos. Chem. Phys., 7, 2057–2071, 2007, http://www.atmos-chem-phys.net/7/2057/2007/. 14572, 14573, 14578

Kroll, J. H., Chan, A. W. H., Ng, N. L., Flagan, R. C., and Seinfeld, J. H.: Reactions of semivolatile organics and their effects on secondary organic aerosol formation, Environ. Sci. Technol., 41, 3545–3550, 2007. 14573

Lack, D. A., Tie, X. X., Bofinger, N. D., Wiegand, A. N., and Madronich, S.: Seasonal variability of secondary organic aerosol: A global modeling study, J. Geophys. Res., 109, D03203, doi:10.1029/2003JD003418, 2004. 14572

Liao, H., Henze, D. K., Seinfeld, J. H., Wu, S., and Mickley, L. J.: Biogenic secondary organic aerosol over the United States: Comparison of climatological simulations with observations, J. Geophys. Res., 112, D06201, doi:10.1029/2006JD007813, 2007. 14576, 14577, 14584

Lightfoot, P. D., Cox, R. A., Crowley, J. N., Destriau, M., Hayman, G. D., Jenkin, M. E., Moortgat, G. K., and Zabel, F.: Organic Peroxy-Radicals - Kinetics, Spectroscopy and Tropospheric Chemistry, Atmos. Environ., 26, 1805–1961, 1992. 14577

Liu, H. Y., Jacob, D. J., Bey, I., and Yantosca, R. M.: Constraints from Pb-210 and Be-7 on wet deposition and transport in a global three-dimensional chemical tracer model driven by assimilated meteorological fields, J. Geophys. Res., 106, 12 109–12 128, 2001. 14578

Martin-Reviejo, M. and Wirtz, K.: Is benzene a precursor for secondary organic aerosol?, Environ. Sci. Technol., 39, 1045–1054, 2005. 14571, 14573

Ng, N. L., Kroll, J. H., Chan, A. W. H., Chhabra, P. S., Flagan, R. C., and Seinfeld, J. H.: Secondary organic aerosol formation from m-xylene, toluene, and benzene, Atmos. Chem. Phys., 7, 3909–3922, 2007, http://www.atmos-chem-phys.net/7/3909/2007/. 14571, 14572, 14573, 14574, 14575, 14578, 14583, 14591

Odum, J. R., Hoffmann, T., Bowman, F., Collins, D., Flagan, R. C., and Seinfeld, J. H.: Gas/particle partitioning and secondary organic aerosol yields, Environ. Sci. Technol., 30, 2580–2585, 1996. 14571, 14572, 14574, 14582

Odum, J. R., Jungkamp, T. P. W., Griffin, R. J., Forstner, H. J. L., Flagan, R. C., and Seinfeld,

J. H.: Aromatics, reformulated gasoline, and atmospheric organic aerosol formation, Environ. Sci. Technol., 31, 1890–1897, 1997. 14571, 14572, 14574, 14582

Offenberg, J. H., Kleindienst, T. E., Jaoui, M., Lewandowski, M., and Edney, E. O.: Thermal properties of secondary organic aerosols, Geophys. Res. Lett., 33, L03816, doi:10.1029/2005GL024623, 2006. 14578

Olivier, J. G. J., Bouwman, A. F., Van der Maas, C. W. M., Berdowski, J. J. M., Veldt, C., Bloos, J. P. J., Visschedijk, A. J. H., Zandveld, P. Y. J., and Haverlag, J. L.: Description of EDGAR Version 2.0: A set of global emission inventories of greenhous gases and ozone-depleting substances for all anthropogenic and most natural sources on a per country basis and on 1°×1° grid, Tech. rep., 1996. 14576

Olivier, J. G. J., Bouwman, A. F., Berdowski, J. J. M., Veldt, C., Bloos, J. P. J., Visschedijk, A. J. H., Van der Maas, C. W. M., and Zandveld, P. Y. J.: Sectoral emission inventories of greenhouse gases for 1990 on a per country basis as well as on 1x1 degree, Environmental Science & Policy, 2, 241–264, 1999. 14576

Park, R. J., Jacob, D., Field, B. D., Yantosca, R., and Chin, M.: Natural and transboundary pollution influences on sulfate-nitrate-ammonium aerosols in the United States: implications for policy, J. Geophys. Res., 109, D15204, doi:10.1029/2003JD004473, 2004. 14575

Park, R. J., Jacob, D. J., Kumar, N., and Yantosca, R. M.: Regional visibility statistics in the United States: Natural and transboundary pollution influences, and implications for the Regional Haze Rule, Atmos. Environ., 40, 5405–5423, 2006. 14575

Pathak, R. K., Presto, A. A., Lane, T. E., Stanier, C. O., Donahue, N. M., and Pandis, S. N.: Ozonolysis of α-pinene: parameterization of secondary organic aerosol mass fraction, Atmos. Chem. Phys., 7, 3811–3821, 2007, http://www.atmos-chem-phys.net/7/3811/2007/. 14578, 14584

Presto, A. A. and Donahue, N. M.: Investigation of α-pinene plus ozone secondary organic aerosol formation at low total aerosol mass, Environ. Sci. Technol., 40, 3536–3543, 2006. 14577, 14578, 14582, 14584

Presto, A. A., Hartz, K. E. H., and Donahue, N. M.: Secondary organic aerosol production from terpene ozonolysis. 2. Effect of NO_x concentration, Environ. Sci. Technol., 39, 7046–7054, 2005. 14571

Pun, B. K. and Seigneur, C.: Investigative modeling of new pathways for secondary organic aerosol formation, Atmos. Chem. Phys., 7, 2199–2216, 2007, http://www.atmos-chem-phys.net/7/2199/2007/., 14572, 14584

Song, C., Na, K. S., and Cocker, D. R.: Impact of the hydrocarbon to NO_x ratio on secondary organic aerosol formation, Environ. Sci. Technol., 39, 3143–3149, 2005. 14571, 14572, 14573, 14577

Surratt, J. D., Kleindienst, T. E., Edney, E. O., Lewandowski, M., Offenberg, J. H., Jaoui, M., and Seinfeld, J. H.: Effect of acidity on secondary organic aerosol formation from isoprene, Environ. Sci. Technol., 41, 5363–5369, 2007. 14584

Tsigaridis, K. and Kanakidou, M.: Global modelling of secondary organic aerosol in the troposphere: a sensitivity analysis, Atmos. Chem. Phys., 3, 1849–1869, 2003, http://www.atmos-chem-phys.net/3/1849/2003/. 14572, 14577, 14578, 14581, 14583

Tsigaridis, K. and Kanakidou, M.: Secondary organic aerosol importance in the future atmosphere, Atmos. Environ., 41, 4682–4692, 2007. 14571, 14580, 14581, 14583, 14584

Tsigaridis, K., Krol, M., Dentener, F. J., Balkanski, Y., Lathiere, J., Metzger, S., Hauglustaine, D. A., and Kanakidou, M.: Change in global aerosol composition since preindustrial times, Atmos. Chem. Phys., 6, 5143–5162, 2006, http://www.atmos-chem-phys.net/6/5143/2006/. 14571, 14577

Turpin, B. J. and Lim, H. J.: Species contributions to $PM_{2.5}$ mass concentrations: Revisiting common assumptions for estimating organic mass, Aerosol. Sci. Tech., 35, 602–610, 2001. 14577

van der Werf, G. R., Randerson, J. T., Giglio, L., Collatz, G. J., Kasibhatla, P. S., and Arellano, A. F.: Interannual variability in global biomass burning emissions from 1997 to 2004, Atmos. Chem. Phys., 6, 3423–3441, 2006, http://www.atmos-chem-phys.net/6/3423/2006/. 14576

van Donkelaar, A., Martin, R. V., Park, R. J., Heald, C. L., Fu, T.-M., Liao, H., and Guenther, A.: Model evidence for a significant source of secondary organic aerosol from isoprene, Atmos. Environ., 41, 1267–1274, 2007. 14577

van Noije, T. P. C., Eskes, H. J., Dentener, F. J., Stevenson, D. S., Ellingsen, K., Schultz, M. G., Wild, O., Amann, M., Atherton, C. S., Bergmann, D. J., Bey, I., Boersma, K. F., Butler, T., Cofala, J., Drevet, J., Fiore, A. M., Gauss, M., Hauglustaine, D. A., Horowitz, L. W., Isaksen, I. S. A., Krol, M. C., Lamarque, J. F., Lawrence, M. G., Martin, R. V., Montanaro, V., Muller, J. F., Pitari, G., Prather, M. J., Pyle, J. A., Richter, A., Rodriguez, J. M., Savage, N. H., Strahan, S. E., Sudo, K., Szopa, S., and van Roozendael, M.: Multi-model ensemble simulations of tropospheric NO_2 compared with GOME retrievals for the year 2000, Atmos. Chem. Phys., 6, 2943–2979, 2006,

http://www.atmos-chem-phys.net/6/2943/2006/. 14583
Volkamer, R., Klotz, B., Barnes, I., Imamura, T., Wirtz, K., Washida, N., Becker, K. H., and Platt, U.: OH-initiated oxidation of benzene – Part I. Phenol formation under atmospheric conditions, Phys. Chem. Chem. Phys., 4, 1598–1610, 2002. 14578
Volkamer, R., Jimenez, J. L., San Martini, F., Dzepina, K., Zhang, Q., Salcedo, D., Molina, L. T., Worsnop, D. R., and Molina, M. J.: Secondary organic aerosol formation from anthropogenic air pollution: Rapid and higher than expected, Geophys. Res. Lett., 33, L17811, doi:10.1029/2006GL02689, 2006. 14571, 14582
Wang, Y. H., Jacob, D. J., and Logan, J. A.: Global simulation of tropospheric O-3-NOx-hydrocarbon chemistry 1. Model formulation, J. Geophys. Res., 103, 10 713–10 725, 1998. 14578
Wang, Y. X., McElroy, M. B., Martin, R. V., Streets, D. G., Zhang, Q., and Fu, T. M.: Seasonal variability of NO_x emissions over east China constrained by satellite observations: Implications for combustion and microbial sources, J. Geophys. Res., 112, D06301, doi:10.1029/2006JD007538, 2007. 14583
Warneke, C., McKeen, S. A., de Gouw, J. A., Goldan, P. D., Kuster, W. C., Holloway, J. S., Williams, E. J., Lerner, B. M., Parrish, D. D., Trainer, M., Fehsenfeld, F. C., Kato, S., Atlas, E. L., Baker, A., and Blake, D. R.: Determination of urban volatile organic compound emission ratios and comparison with an emissions database, J. Geophys. Res., 112, D10S47, doi:10.1029/2006JD007930, 2007. 14584
Wesely, M. L.: Parameterization of Surface Resistances to Gaseous Dry Deposition in Regional-Scale Numerical-Models, Atmos. Environ., 23, 1293–1304, 1989. 14578
Zhang, Y., Huang, J.-P., Henze, D. K., and Seinfeld, J. H.: The role of isoprene in secondary organic aerosol formation on a regional scale, J. Geophys. Res., 112, D06201, doi:10.1029/2006JD007813, 2007. 14577
Zhao, J., Zhang, R. Y., Misawa, K., and Shibuya, K.: Experimental product study of the OH-initiated oxidation of m-xylene, J Photoch Photobio A, 176, 199–207, 2005. 14573

Table 1. Stoichiometric coefficients, $\alpha_{i,j}$, and equilibrium partitioning coefficients, $K_{i,j}$, for SOA formation derived from high and low-NO_x chamber experiments of reaction of aromatics with OH (Ng et al., 2007). The reference temperature for the $K_{i,j}$'s is 295 K.

Parent aromatic i	$\alpha_{i,H}$	$\alpha_{i,1}$	$\alpha_{i,2}$	$K_{i,1}$ [$m^3\ \mu\ g^{-1}$]	$K_{i,2}$ [$m^3\ \mu\ g^{-1}$]
benzene	0.2272	0.0442	0.5454	3.3150	0.0090
toluene	0.2349	0.0378	0.0737	0.4300	0.0470
m-xylene	0.2052	0.0212	0.0615	0.7610	0.0290

Table 2. Reaction rate constants, $k = Ae^{B/T}$.

Reaction	Rate constant[a]	k_{298} [cm^3 molec^{-1}s^{-1}]	A [cm^3 molec^{-1}s^{-1}]	B [K]
(R1)	$k_{OH,B}$	1.22×10^{-12}	2.33×10^{-12}	−193
(R1)	$k_{OH,T}$	5.63×10^{-12}	1.81×10^{-12}	338
(R1)	$k_{OH,X}$	2.31×10^{-11}	2.31×10^{-11}	0
(R2)	k_H	1.5×10^{-11}	1.4×10^{-12}	700
(R3)	k_N	8.5×10^{-12}	2.6×10^{-12}	350

[a]B = benzene, T = toluene, X = xylene. Constants k_H and k_N assumed equal for each parent aromatic.

Table 3. Emission ratios for biofuel and biomass burning sources of aromatic species (mmoles emitted per mole CO emitted) taken from Andreae and Merlet (2001) with updates from M. O. Andreae (personal communication, 2006).

Aromatic species	Biofuel burning	Biomass burning
benzene	4.06	2.33
toluene	2.01	1.24
xylene	0.82	0.48

Table 4. Emissions of each aromatic species broken down by source [Tg C /yr].

Aromatic species	Industrial and fossil fuel	Biofuel burning	Biomass burning
benzene	1.3	1.8	2.5
toluene	4.3	1.0	1.6
xylene	3.5	0.5	0.7

ACPD
7, 14569–14601, 2007

Table 5. Global SOA budgets.

Hydrocarbon	Emission (Tg/yr)	SOA Production (Tg/yr)	Burden (Tg)
terpenes	121	8.2	0.21
alcohols	38.3	1.5	0.03
sesquiterpenes	14.8	2.0	0.03
isoprene	461	13.2	0.43
aromatics	18.8	3.5	0.08
total	654	28.4	0.78

ACPD
7, 14569–14601, 2007

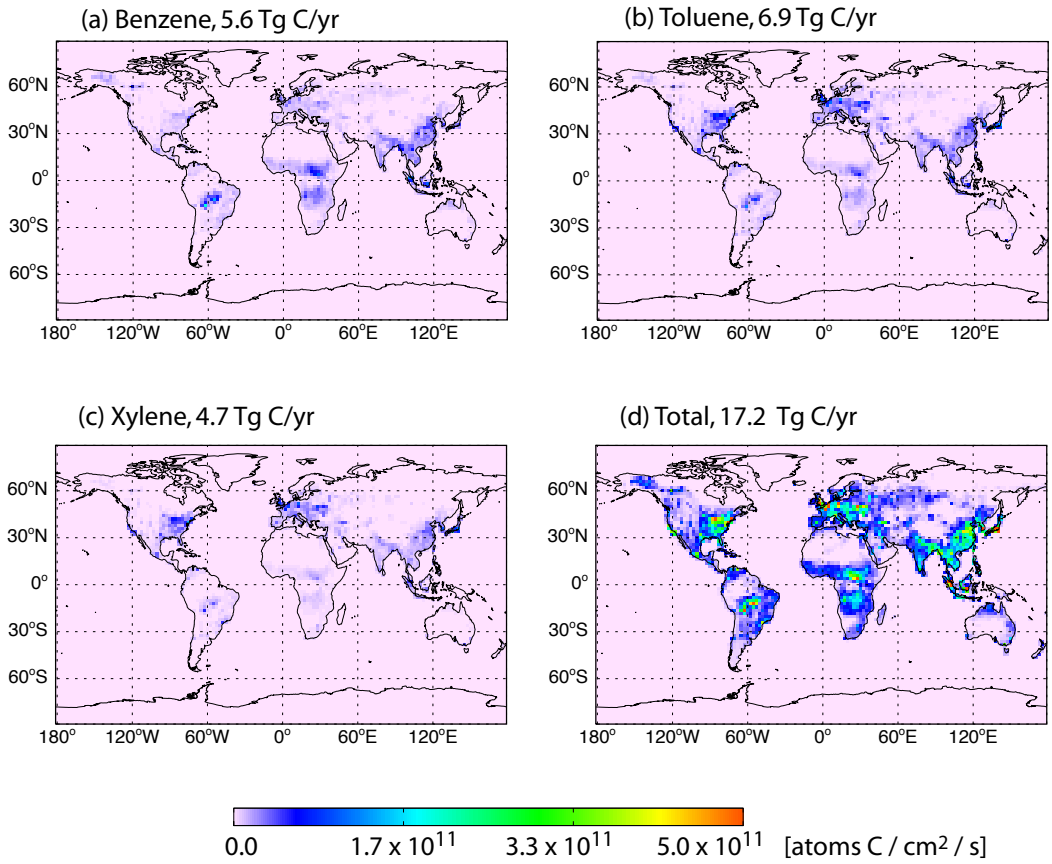

Fig. 1. Emissions of aromatic compounds.

ACPD
7, 14569–14601, 2007

EGU

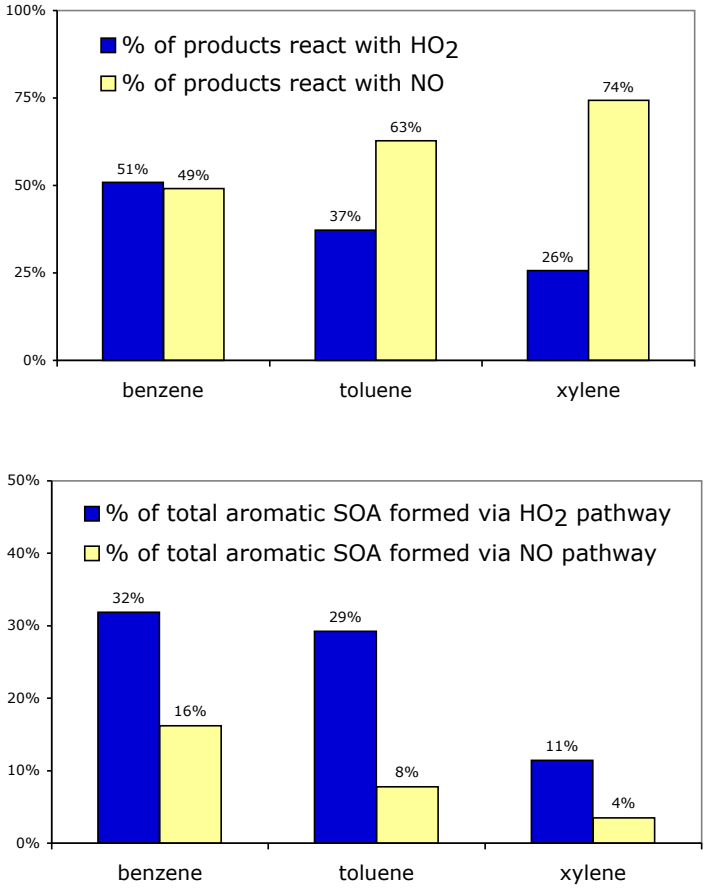

Fig. 2. Percentages of peroxy radical from each parent aromatic that react with HO_2 radical (R2) vs with NO (R3) and the eventual contributions from each pathway to the total SOA production from all aromatic species.

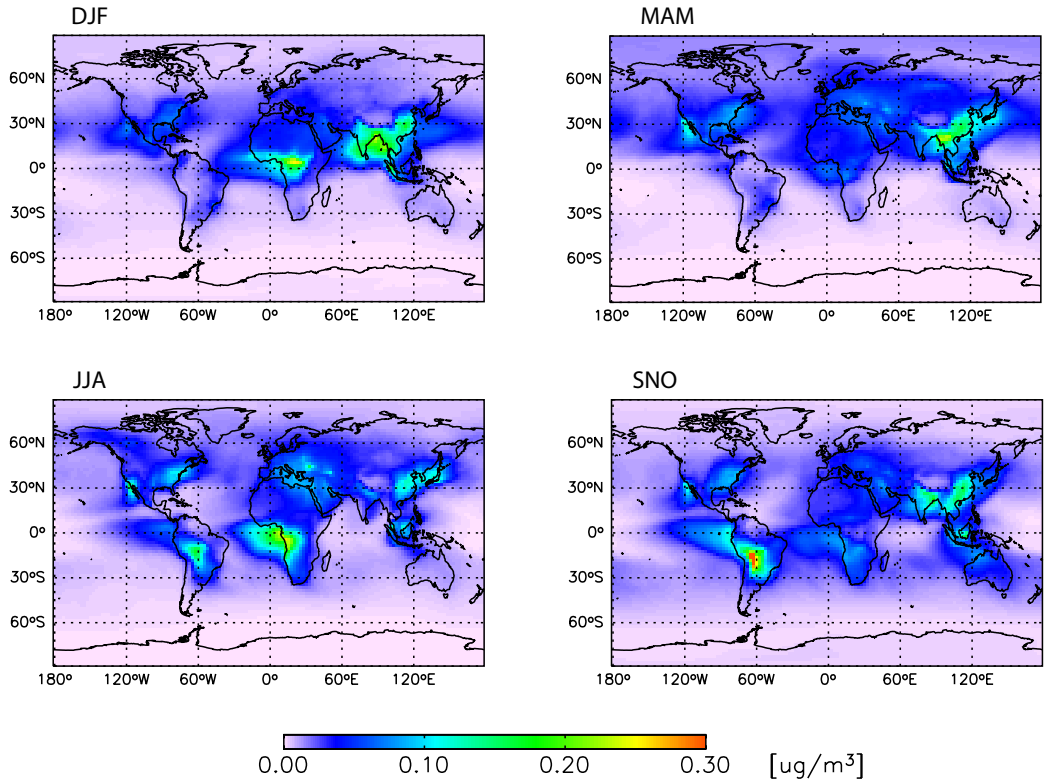

Fig. 3. Seasonal distributions of the total surface-level SOA concentrations from benzene, toluene and xylene.

ACPD
7, 14569–14601, 2007

EGU

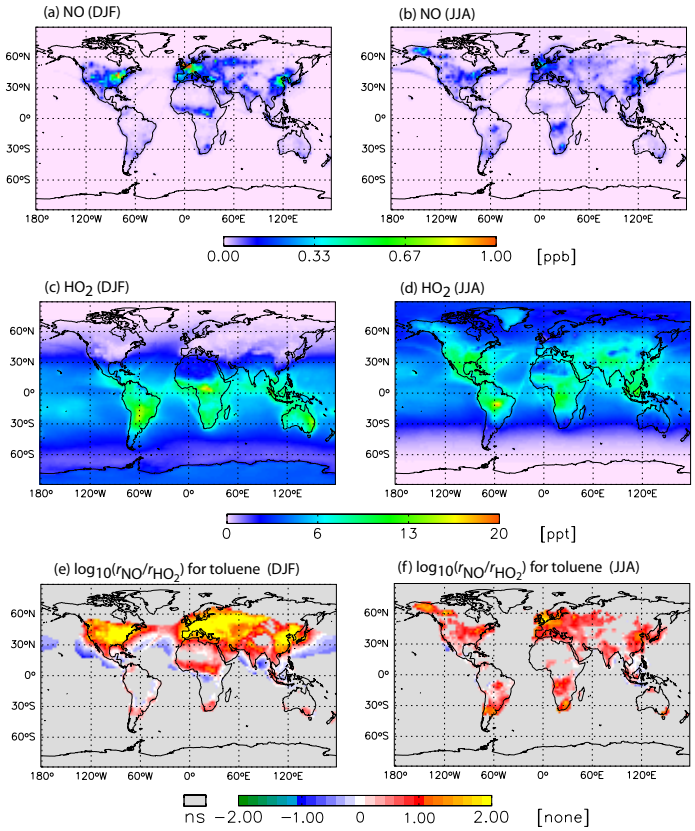

Fig. 4. Panels **(a–d)** are the seasonally averaged surface-level concentrations of NO and HO_2. Panels **(e)** and **(f)** show the log of the resulting branching ratio between reaction of the toluene peroxy radical with NO vs reaction with HO_2. Not shown are values where net reacted peroxy radical is <1% of the surface-level maximum. Comparing results in the Eastern United States and Europe, both decreased NO and increased HO_2 during JJA lead to increased reaction via the low-NO_x (high-yield) pathway.

ACPD
7, 14569–14601, 2007

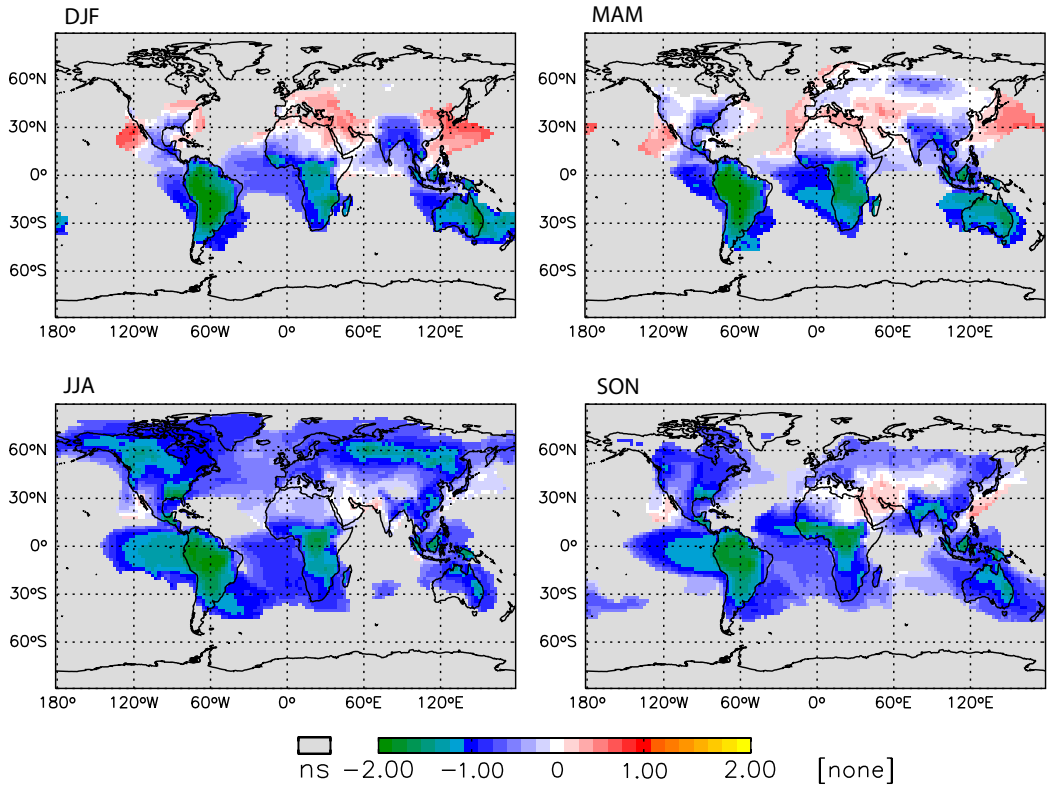

Fig. 5. The log of the ratio of seasonally averaged surface concentrations of anthropogenic to biogenic SOA, $\log_{10}\left(\frac{[\mathrm{SOA}_{\mathrm{arom}}]}{[\mathrm{SOA}_{\mathrm{biogenic}}]}\right)$, omitting values where the total SOA concentration is less than $0.05\,\mu\mathrm{g/m}^3$. For simplicity, biomass burning sources of aromatics are considered to be anthropogenic.

ACPD
7, 14569–14601, 2007

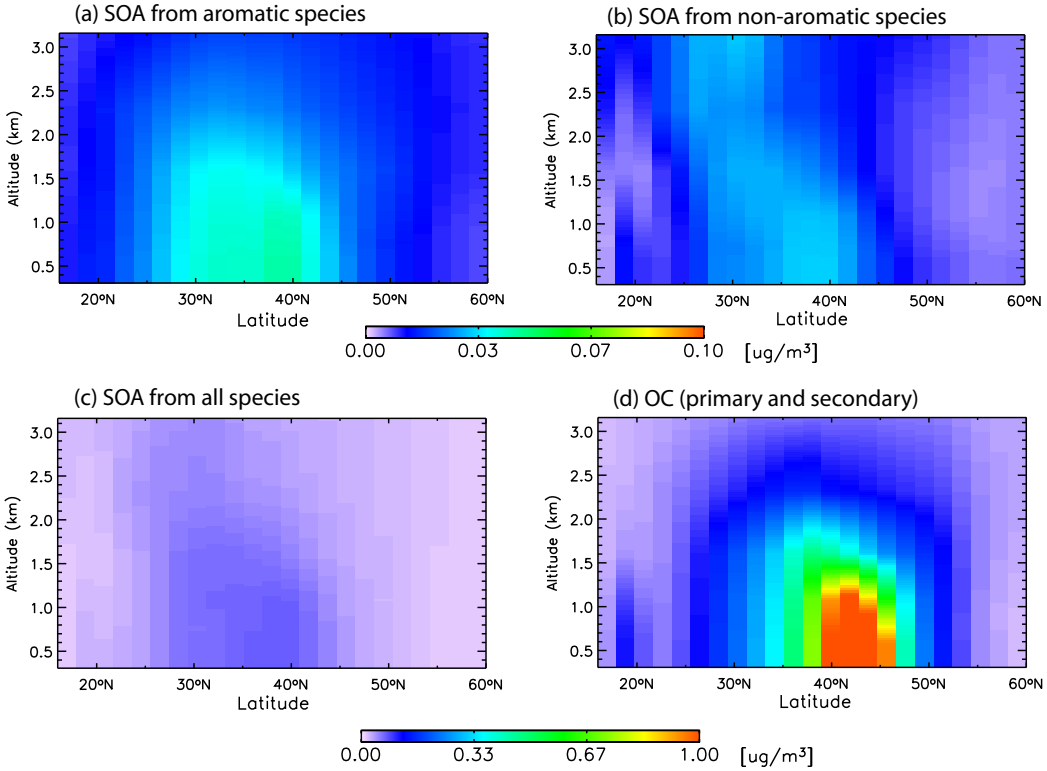

Fig. 6. A profile of SOA concentrations at 70° W (east of the United States) during DJF. Panels **(a)** and **(b)** show the linear contributions from anthropogenic and biogenic sources, respectively. Noting the change in scale, panels **(c)** and **(d)** show the total SOA from all sources and the total organic carbon aerosol from primary and secondary sources.

ACPD
7, 14569–14601, 2007

EGU